Directed Organization of Platinum Nanocrystals through Organic Supramolecular Nanoporous Templates

Farid Kameche, Alice Six, Fabrice Charra, Anh-Tu Ngo, Fabrice Mathevet, Caroline Salzemann, David Kreher, Imad Arfaoui, André-Jean Attias, Christophe Petit

Directed organization of platinum nanocrystals through organic supramolecular nanoporous templates.

Farid Kameche [1,2,3], Alice Six[2], Fabrice Charra[3], Anh-Tu Ngo[1], Fabrice Mathevet [2], Caroline Salzemann[1], David Kreher [2], Imad Arfaoui[1],André-Jean Attias[2,], Christophe Petit[1,]**

1) Sorbonne Universités, UPMC Univ Paris 06, MONARIS, UMR CNRS 8233, 4 Place Jussieu, 75252 Paris Cedex 05, France.

2) Sorbonne Universités, UPMC Univ Paris 06, Institut Parisien de Chimie Moléculaire, UMR CNRS 8232, 4 Place Jussieu, 75252 Paris Cedex 05, France.

3) Service de Physique de l'Etat Condensé, CEA CNRS Université Paris-Saclay, CEA Saclay F-91191 Gif-sur-Yvette CEDEX, France.

Abstract

We propose a novel approach to trap 2 nm Pt nanocrystals using nanoporous two-dimensional supramolecular networks for cavity-confined host-guest recognition process. This will be achieved by taking advantage of two features of supramolecular self-assembly at surfaces. First, its capability to allow to the formation of complex 2D architectures, more particularly nanoporous networks, through non-covalent interactions between organic molecular building-blocks. Second, the ability of the nanopores to selectively host and immobilize a large variety of guest species. In this paper, for the first time, we will use isotropic honeycomb networks and anisotropic linear porous supramolecular networks to host 2nm Pt nanocrystals.

Keywords*: directed organizations, nanocrystals, supramolecular templates, self-assemblies at surfaces, nanoporous networks*

1- Introduction

Widely studied, metallic nanoparticles (NPs) present a plethora of interesting intrinsic properties (optical, magnetic, catalytic, electronic…).[1–6] However, a precise control over their spatial organization on different length scale is essential to steer the particles interactions to improve the performance of the next generation of materials (i.e., for spintronics, plasmonics) and devices (i.e., sensors, high density data storages memories,..). In this regards, both properties and performances may be enhanced by controlling finely the positional order within a two-dimensional (2D) self-assembly. [7,8] However, this is still a real challenge for NPs smaller than 3nm in diameter. Indeed, the driving forces explaining the formation of self-assemblies of colloidal NPs surrounding by capping molecules, are well known.[9-11] It consists in different contributions to the NP-NP interactions including van der Waals (vdW) attractive forces between the cores and/or the passivating chains, mostly alkyl chains, as well as osmotic, electrostatic and elastic contributions. On the one hand, the size of the nanocrystals has to be large enough (typically diameter ≥ 3 nm) to favor vdW interactions. On the other hand, the balance between capping agent elastic repulsion and attractive vdW forces controls the interparticle distance. It is important to stress that capping agent-mediated interparticle interactions are sensitive to factors such as solvent, temperature, bonding strength, coating thickness. Anyhow the control of the interparticle distance by changing the alkyl chain length is limited, [7] it is therefore difficult to control both long-range organization and interparticle spacing, especially in the case of 2D assemblies where the effects of substrate can be predominant. [10] However, to develop devices based on these assemblies, it is necessary to be

able to adjust these two parameters easily and in particular to control the interactions between nanoparticles within the periodic networks.

Thus, in order to go further in the integration of nanoparticles in usable systems, another approach that allows both to control the organization at very long distance and to modulate the interactions between nano-objects has to be develop, especially for NPs smaller than 3 nm. Hence, pre-patterning the substrate appears as an efficient way to direct the organization of 2D-confined NPs and to control both the interparticle distances and the geometry of the NPs assembly. For example, a fine tuning of molecule-substrate forces based on complementary H-bonding functionalization of the particle and the substrate could be usefull to overcome the problem, as it has been demonstrated for Au_{55} nanocrystals (NCs).[12] Hence, pre-patterning the substrate appears as an efficient way to direct the organization of 2D-confined NPs and to control both the interparticle distances and the geometry of the NPs assembly. This pre-patterning can also itself result from the self-assembly of third-party molecules. For example, the lamellae formed by the self-assembly of linear alkanes or their derivatives on atomically-flat crystal surfaces can act as rails which drive the alignment of NPs.[13,14] However, in these systems, the interparticle distance (around 2 nm) along the rail remained very small which could be a critical technological limitation for application as high density data storage.[4,5,15]

On the other hand, the progress in supramolecular self-assembly at surfaces allows towards the formation of more complex nanostructures with controlled topologies. [16,17] In previous work, we developed a functional group (so called 'clip') for supramolecular bonding by interdigitation of the alkyl chains on sp_2 carbon-based substrates[18] (e.g. highly-oriented pyrolytic graphite (HOPG) and graphene) (**Chart 1**). We demonstrated that 1,3,5-tristyrylbenzene substituted in positions 3 and 5 by alkoxy peripheral chains presenting n=6, 8, 10, 12, or 14 carbon atoms (**TSB3,5-C$_n$**) can form a series of isotropic nanoporous

honeycomb networks were the cavity diameter and cavity-cavity distances can be tuned by playing with the alkyl chain length.[18,19] Moreover, the ability of these 2D structures to trap disk-shapes molecules has been demonstrated.[20] Moreover, the topology of the 2D porous network can be changed by replacing the above star shape molecules bearing 3 clips, with molecules bearing 2 clips like the first generation conjugated dendrimer (**G1-DSB-C$_n$**) consisting of a distyrylbenzene core, stilbene dendrons, and alkoxy terminal chains (Cn), which forms anisotropic nanoporous networks. [18,21]

Here, we propose a novel approach based on nanoporous 2D supramolecular networks for cavity-confined host-guest recognition process. This will be achieved by taking advantage of two features of supramolecular self-assembly at surfaces. First, its capability to allow to the formation of complex 2D architectures, more particularly nanoporous networks, through non-covalent interactions between organic molecular building-blocks (tectons). Second, the ability of the nanopores to selectively host and immobilize a large variety of guest species.[22,25] In this paper, for the first time, we will use isotropic honeycomb networks and anisotropic linear porous supramolecular networks to host 2nm Pt nanocrystals. More precisely, in a first stage, the supramolecular templates are built at liquid /solid interface by supramolecular self-assembly on highly oriented pyrolytic graphite (HOPG) and characterized by scanning tunneling microscopy (STM). Then, in a second stage, the nanoparticles are deposited by solvent evaporation on the patterned substrates. We will demonstrate by High Resolution scanning electron microscopy (HRSEM) that the nanopatterning of the substrate by porous networks controls the organization (distance and geometry) of 2nm metallic NCs.

2- Results and Discussions

To demonstrate the host–guest concept for directed assembly of NCs, a series of porous templates have been investigated. They consist of anisotropic and isotropic networks

obtained from tectons **G1-DSB-C$_{14}$** and **TSB3,5-C$_{12}$ (Chart 1),** respectively. To address the limitation on interparticles distances reported above, according to our previous results [21] the tectons **G1-DSB-C$_{14}$** with the longer alkoxy peripheral C14 chains was chosen in order to increase the spacing between the pores (4.4 nm) and thus the interparticle distances. Experimental STM image (**Figure 1A$_1$**) of **G1-DSB-C$_{14}$** supramolecular assembly confirms the formation of an anisotropic linear porous network [21] this corresponds to the so called 'regular' configuration. The lattice parameters extracted from **Figure 1A$_1$** are reported and superimposed on the molecular scheme (**Figure 1A$_2$**). Beyond this regular arrangement**,** **Figure 1B$_1$** show that self-assembly is subjected to the formation of defects. In particular, a shift along the molecular lamellae can occur, resulting in a variant in clipping geometry in addition to the low-high interdigitation present in the regular pattern. This second arrangement named 'gauche' corresponds to the high-low interdigitation (i.e., an inversion of the clips). It is less common but visible on **Figure 1B$_1$** and **B$_2$** where it induces stacking faults. This predominance of the regular configuration can be interpreted by a better stacking stabilization. Such packing faults can appear either as a junction between two neighboring mismatched domains grown independently, or as the defective growth of a domain following the accidental misplacement of an initial **1-DSB-C$_{14}$** molecule in a gauche configuration.[21]

Regarding the isotropic network, the **TSB-3,5-C$_{12}$** tecton has been chosen because it can form a honeycomb network the pore diameter of which (1.9 nm) is commensurate with the size of the NCs (2 nm).[19] However, it has been reported that the tecton **TSB-3,5-C$_{12}$** could self-assemble along various schemes depending on concentration and temperature.[19] At room temperature, below the critical concentration C_C=10^{-3} mol.L^{-1}, a honeycomb structure is formed (**Figure 1C$_1$ and 1C$_2$**). Above C_C, a dense organization is observed (linear organization α) together with a second linear organization (linear organization β, **Figure 1D$_1$ and 1D$_2$**). Their geometrical parameters are summarized in **Table 1**. The orientation of

the underlying HOPG lattice has been obtained from the angle formed by mirror-symmetrical molecular domains, following the method detailed in ref. [19]. Concerning the last one (β), although the location of the aromatic core is accurately determined from STM images, the position of the alkoxy peripheral chains against the substrate is less clear, as illustrated on **Figure 1D$_2$**. These STM images of the molecular template have been acquired at the liquid-solid interface, which offers a better stability and resolution through the rejection of surface contaminants that are insoluble in phenyloctane. However, the same organization is obtained after removal of a volatile solvent such as toluene, although its dry STM imaging is less convenient (images given in online supplementary material, figure S3 and S4)".

The platinum nanoparticles were synthesized according to the liquid-liquid phase transfer method (Supporting Information). [26-28] This method allows the synthesis of NCs with various size distributions. We chose to focus on 2 nm Pt nanoparticles for two reasons. Firstly, this would permit to emphasize the difference between the poor local organization of free NC assembly and that directed by the supramolecular template. Secondly, the size of the nanocrystals matches that of the two honeycomb network pores, which is supposed to favor their trapping. Nevertheless, the results presented here are not specific to the nature of the metal chosen. We synthesized 2 nm Pt nanocrystals with a polydispersity close to 12%, (Figure S5 and S6) stabilized by oleylamine stabilizing agent and dispersed in chloroform (referred to as Pt-$C_{18}NH_2$).

In order to study the effect of the supramolecular template on the NCs organization, we compared two preparation procedures with a control sample. To reach this goal, three solutions were prepared: a 2×10^{-6} mol.L^{-1} solution of **G1-DSB-C$_{14}$** in phenyloctane (solution 1), a 1×10^{-6} mol.L^{-1} solution of **TSB-3,5-C$_{12}$** in phenyloctane (solution 2) - the concentration was determined to promote the formation of the honeycomb structure - and a 1×10^{-6} mol.L^{-1} solution of Pt-$C_{18}NH_2$ in chloroform (solution 3). To consider the effect of the isotropic

template, first 10 µL of solution 1 was deposited on a freshly cleaved graphite heated at 60°C during 10 minutes. After a few hours, the phenyloctane is evaporated and 10 µL of solution 3 is added. Dried, the sample was characterized by HRSEM. To consider the effect of the anisotropic template, a second sample was prepared in the same way but by replacing solution 1 with solution 2. A control sample was prepared using the solution 3 only (Supporting Information, figure S7). We consider that all the molecules and nanoparticles are dropped on the surface with no loss. Contrarily to the control sample (NPs deposited on raw HOPG, figure S7), where only a local organization barely exists, the nanoparticles present a periodic arrangement, when using an organized porous template (**Figure 2 and Figure 3).** EDX analysis of the sample, after deposition of the nanoparticles solution and evaporation of the solvent, shows that only carbon and platinum are present on the substrate (See Figure S8). This confirms that the spherical nano-object deposited on the substrate could only be platinum nanocrystals. To evidence the patterning effect, 2D digital fast Fourier transform (2D-FFT) was applied to HRSEM allowing the determination of the experimental lattice parameters and the analysis of any possible commensurability with the supramolecular template.

For the isotropic template of **G1-DSB-C_{14}** molecules**,** a typical HRSEM image of Pt-$C_{18}NH_2$ nanocrystals is shown **figure 2A**. It reveals a hexagonal organization of the metallic NPs. A zoom in this image (**Figure 2B**) and more particularly its FFT (**Figure 2C**) emphasizes the presence of a quasi-hexagonal lattice with $A_{1,exp}$ = 4.1 nm, $B_{1,exp}$ = 4.46 nm and $C_{1,exp}$= 4.65 nm. This periodicity matches a model in which every second pore is filled along the $\mathbf{a_1}$ direction whereas all the pores are filled on the $\mathbf{b_1}$ direction of the **G1-DSB-C_{14}** network (**Figure 2D**). At some specific places of the same sample, an organization close to the quasi-hexagonal one has been observed and is present on **Figure 3A** and **Figure 3B**. However, four periods are revealed by the FFT (**Figure 3C**), $A_{2,exp}$ = 4.02 nm, $B_{2,exp}$ = 4.5 nm, $C_{2,exp}$= 4.68 nm and $D_{2,exp}$ = 5.22 nm. The three first values, $A_{2,exp}$, $B_{2,exp}$ and $C_{2,exp}$, are close

to $A_{1,exp}$, $B_{1,exp}$ and $C_{1,exp}$ and are thus interpreted by the same organization. Yet, $D_{2,exp}$ cannot be explained with the ideal model proposed on **Figure 2D**. Nonetheless, the value $D_{2,exp}$ may be related to gauche configurations (**Figure 1B**), as represented on **Figure 3B**, which shows that the theoretical value D_2 fits well with the experimental one $D_{2,exp}$. Hence, these results implies that the NCs organization is directed by the molecular patterns of organic molecules deposited on HOPG. Indeed, not only the perfect organization of the supramolecular template (**Figure 1A**), but also the defects (**Figure 1B**) can be reproduced by the 2D assembly of metallic NCs. Thus, the present results show a directed assembly of metallic NCs induced by a supramolecular template. On **Figure 2D** and **3D**, the Pt-$C_{18}NH_2$ nanocrystals are supposedly positioned on the pores of the template. Yet, establishing the real position of the nanocrystals compared to the **G1-DSB-C_{14}** network is still delicate, even with HRSEM and STM. In the case of gold NCs on lamellar templates completely covering HOPG,[13] it has been speculated that NCs interact with the aromatic core of the molecules and were then localized on it. Here, both **G1-DSB-C_{14}** molecules and the substrate are accessible to the NCs and present an aromatic character. Thus, we cannot determine the correct position of the nanocrystals compared to the supramolecular template.

Concerning the anisotropic template, using exactly the same protocol, a sample was obtained by substituting **G1-DSB-C_{14}** with **TSB-3,5-C_{12}**. The corresponding HRSEM image is presented on **Figure 4A**. Once zoomed (**Figure 4B**) and thanks to a FFT (**Figure 4C**), a surprising regularity is observed which may indicate that nanocrystals are aligned on an oblique lattice with $A_{3,exp}$ = 5.2 nm, $B_{3,exp}$ = 5.8 nm and $\Gamma_{3,exp}$ = 82°. The concentration of the solution of TSB-3,5-C_{12} is adjusted so as to form honeycomb lattices when the sample is dried. However, we observe no clear correlation between the oblique lattice of the nanoparticles and the honeycomb lattices of the TSB-3,5-C_{12}. Nonetheless, in practice, during the deposition of the TSB-3,5-C_{12} solution and the evaporation of phenyloctane, the local concentration of the

TSB-3,5-C_{12} molecules is not the same on all the substrate. These hypothesis, which are supported by experimental results obtained on a dried sample (see Supporting Information **Figure S3**), allow us to consider other possible organizations observed for TSB-3,5-C_{12} molecules self-assembled on graphite. As already mentioned, a correlation may exist between experimental results and the linear organization β. In contrast with what observed with **G1-DSB-C_{14}** molecules, here the NPs can be tentatively placed according to the direction of the vector $2\mathbf{a_2}+0.5\mathbf{b_2}$ and $-\mathbf{a_2}+\mathbf{b_2}$, as shown on **Figure 4D**. Contrarily to the previous experiments, there are no pores on the linear organization β to welcome the NCs. According to the observation done before on the relative position of the Pt NCs with the **G1-DSB-C_{14}** molecules, we might then think that the presence of an aromatic core is a necessary and sufficient condition to get a direct assembly of metallic NCs. However, due to the unknown position of the alkoxy peripheral chains on the linear organization β, we cannot exclude a possible interaction between them and the stabilizing agent that influence the direct assembly. As a matter of fact, if the alkoxy chains are effectively oriented out of the plane of the template, we can imagine that they may interact with the oleylamine physisorbed on the Pt NCs surface.

3- Conclusion

To summarize, these studied demonstrates validate the host-guest concept for directed assemblies of metallic NPs smaller than 3 nm in diameter, which usually barely self-organize. This is testified by the differences observed in NP organization between the control sample (without molecular patterns) and the samples modified with supramolecular templates. More particular, the effect of the supramolecular template was clearly highlighted by the imprint of the templates defects on the nanocrystals organization. The control of the interparticles distances and the geometry of the network of NPs lead to imagine different use of this system

especially for high-density magnetic recording by using highly magnetic NCs as CoPt nanoalloys with similar size.[26]

Acknowledgements

This work was supported by the French ANR within the program ‘‘NANOCRISNET’’ under Contract ANR-11-BS10-018 and by C’Nano Ile-de-France. AJA thanks AOARD. We are also grateful to the ‘‘Service Commun de Microscopie de l’UFR de Chimie de l’UPMC’’ and to D. Montero for the HRSEM characterization of the samples.

Supporting Information

Supporting Informations are available.

References

[1] Anker, J. N.; Hall, W. P.; Nilam, O. L.; Shah, C., J. Zhao, R. P. Van Duyne, R. P. Biosensing with plasmonic nanosensors, *Nature Materials* **2008**, *7*, 442-453.

[2] Wang, X.; Choi, S-I.; Roling, L. T.; Luo, M. ; Ma, C. ; Zhang, L.; Chi, M. ; Liu, J. ; Xie, Z. ; Herron, J. A.; Mavrikakis, M. ; Xia, Y. Palladium–platinum core-shell icosahedra with substantially enhanced activity and durability towards oxygen reduction, *Nature Communications* **2015**, *6*, 7594-7602.

[3] Choi, J-H.; Wang, H.; Oh. S. J.; Paik, T.; Jo, P. S.; Sung, J.; Ye, X.; Zhao, T.; Diroll, B. T.; Murray, C. B.; Kagan, C. R. Exploiting the colloidal nanocrystal library to construct electronic devices, *Science*, **2016**, 352, 205-208.

[4] Alloyeau, D.; Mottet, C.; Ricolleau, C.; Eds., *Nanoalloys*, Springer London, London, **2012**.

[5] Calvo, F., Ed., *Nanoalloys: From Fundamentals to Emergent Applications*, Elsevier, Amsterdam, **2013**.

[6] Frey, N. A.; Peng, S.; Cheng, K. and Sun, S.; Magnetic nanoparticles: synthesis, functionalization, and applications in bioimaging and magnetic energy storage. *Chem. Soc. Rev.*, **2009**, *38*, 2532-2542.

[7] Pileni, M.-P. Nanocrystal Self-Assemblies: Fabrication and Collective Properties, *J. Phys. Chem. B,* **2001***, 105,* 3358-3371.

[8] Pileni, M. P. Supracrystals of Inorganic Nanocrystals: An Open Challenge for New Physical Properties, *Acc. Chem. Res.* **2008**, *41*, 1799.

[9] Boles, M. A.; Engel, M.; Talapin, D. V. Self-Assembly of Colloidal Nanocrystals: From Intricate Structures to Functional Materials *Chem. Rev*. **2016**, *116*, 11220–11289.

[10] Motte, L. ; Lacaze, E. ; Maillard, M.; Pileni, M. P. ; Self-Assemblies of Silver Sulfide Nanocrystals on Various Substrates, *Langmuir* **2000**, *16*, 3803–3812.

[11] Brune, H.; Courty, A.; Petit, C.; and Repain, V.; « Self-assembly of nano-alloys » *in Nanoalloys: From Fundamentals to Emergent Applications*, Florent Calvo, Editors, Elsevier **2013**, Chapter 11, 373.

[12] Schmid, G.; Bäumle, M.; Beyer, N. Ordered Two-Dimensional Monolayers of Au55 Clusters, *Angew. Chem. Int. Ed.* **2000**, *39*, 181-183.

[13] Mezour, M. A.; Perepichka, I. I.; Zhu, J.; Lennox, R. B.; Perepichka, D. F. Directing the assembly of gold nanoparticles with two-dimensional molecular networks. *ACS Nano* **2014**, *8*, 2214-2222.

[14] Makarova, M.; Mandal, S. K.; Okawa, Y.; Aono, M. Ordered Monomolecular Layers as a Template for the Regular Arrangement of Gold Nanoparticles, *Langmuir* **2013**, *29*, 7334-7343.

[15] Scholten, P. C.; Tjaden, D. L. A. Mutual attraction of superparamagnetic particles *J. Colloid Interface Sci.* **1980**, *73*, 254-255.

[16] Mali, K. S.; Pearce, N.; De Feyter, S.; Champness, N. R. Frontiers of supramolecular chemistry at solid surfaces. *Chem. Soc. Rev*., **2017**,*46*, 2520-2542.

[17] Barth, J. V.; Costantini G. and Kern, K. Engineering atomic and molecular nanostructures at surfaces, *Nature*, **2005**, *437*, 671-679.

[18] Bléger, D.; Kreher, D.; Mathevet, F.; Attias, A.-J.; Schull, G.; Huard, A.; Douillard, L.; Fiorini-Debuischert, C.; Charra, F. Surface noncovalent bonding for rational design of hierarchical molecular self-assemblies, *Angew. Chem. Int. Ed.* **2007**, *46*, 7404.

[19] Arrigoni, C.; Schull, G.; Bléger, D.; Douillard, L.; Fiorini-Debuisschert, C.; Mathevet, F.; Kreher, D.; Attias, A.-J.; Charra, F. Structure and Epitaxial Registry on Graphite of a Series of Nanoporous Self-Assembled Molecular Monolayers, *J. Phys. Chem. Lett.* **2010**, *1*, 190-194.

[20] Schull, G.; Douillard, L.; Fiorini-Debuisschert, C.; Charra, F.; Mathevet, F.; Kreher, D.; Attias, A.-J.;Single-Molecule Dynamics in a Self-Assembled 2D Molecular Sieve *Nano Lett.* **2006**, *6*, 1360-1363.

[21] Six, A.; Bocheux, A.; Charra, F.; Mathevet, F.; Kreher, D. ; Attias, A.-J. 2D self-assembly of phenylene–vinylene tectons at the liquid–highly oriented pyrolytic graphite interface: from chain length effects to anisotropic guest–host dynamics, *Nanotechnology* **2016**, *28*, 025602.

[22] Bonifazi, D.; Mohnani, S.; Llanes-Pallas, A.; Supramolecular Chemistry at Interfaces: Molecular Recognition on Nanopatterned Porous Surfaces, *Chem. Eur. J.* **2009**, *15*, 7004-7025.

[23] Mali, K. S. ; Adisoejoso, J. ; Ghijsens, E. ; De Cat, I. ; De Feyter, S. Exploring the Complexity of Supramolecular Interactions for Patterning at the Liquid–Solid Interface, *Accounts of Chemical Research* **2012**, *45*, 1309-1320.

[24] Elemans, J. A.; Lei, S.; De Feyter, S. ; Molecular and supramolecular networks on surfaces: from two-dimensional crystal engineering to reactivity, *Angew. Chem. Int. Ed.* **2009**, *48*, 7298-7332.

[25] Sosa-Vargas, L.; Kim, E.; Attias, A. J.; Beyond "decorative" 2D supramolecular self-assembly: strategies towards functional surfaces for nanotechnology *Materials Horizons* **2017** DOI: 10.1039/C7MH00127D

[26] Demortière, A.; Petit, C. First Synthesis by Liquid−Liquid Phase Transfer of Magnetic Co_xPt_{100-x} Nanoalloys *Langmuir* **2007**, *23*, 8575.

[27] Brust, M.; Walker, M.; Bethell, D.; Schiffrin, D. J.; Whyman, R. Synthesis of thiol-derivatised gold nanoparticles in a two-phase Liquid–Liquid system *J. Chem. Soc., Chem. Commun.* **1994**, *7*, 801-802.

[28] Brust, M.; Bethell, D.; Kiely, C. J.; Schiffrin, D. J. Self-Assembled Gold NanoparticleThin Films with Nonmetallic Optical and Electronic Properties. *Langmuir* **1998**, *14*, 5425−5429.

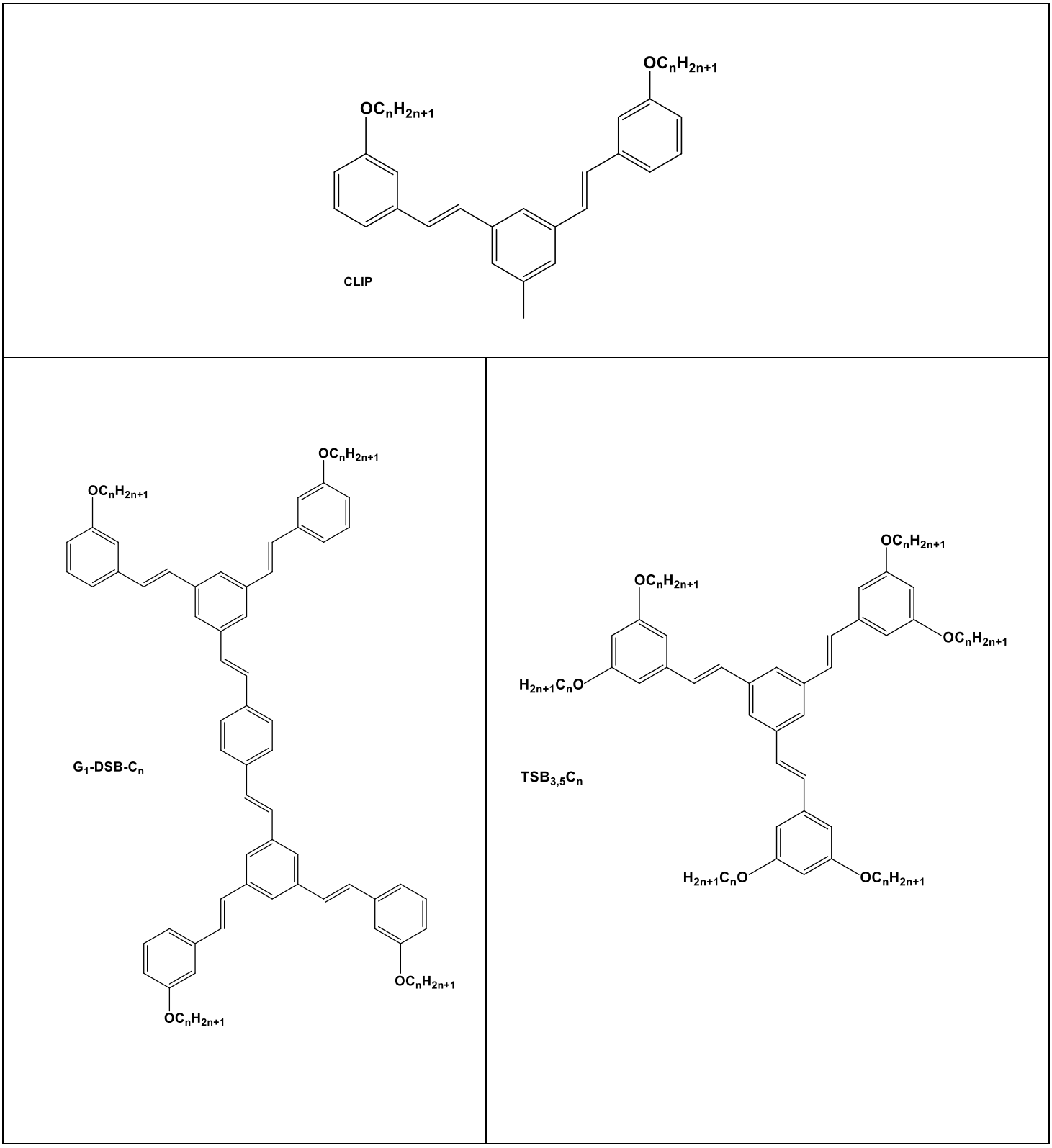

Chart 1 : Molecular structure of the functional group « clip » (top) and the two derivatives used in this work **G1-DSB-C_n** (left) and **TSB3,5-C_n** (right).

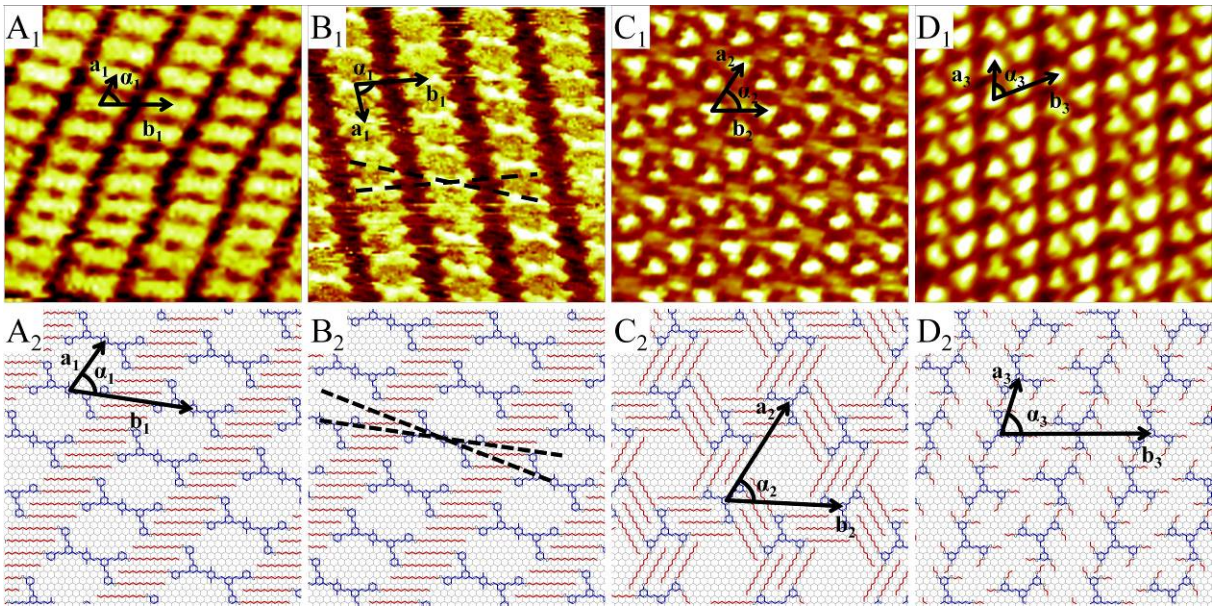

Figure 1. (1) STM images (23x23 nm^2) of (A and B) **G1-DSB-C_{14}** molecules self-assembled on linear network (I=12 pA, V=-680 mV, C=1.0x10^{-4} mol.L^{-1}) and TSB-3,5-C_{12} molecules self-assembled on (C) honeycomb and (D) β compact network (I=20 pA, V=-888 mV, C=4.0x10^{-5} mol.L^{-1}). On the B image, defects are observed and induce a translation along the $\mathbf{a_1}$ direction represented by the black dot lines. For all images, lattices parameters had been determined experimentally and used to determine (2) a representation of the (A and B) **G1-DSB-C_{14}** molecules and the (C and D) TSB-3,5-C_{12} molecules' self-assembly on graphite (a_1=2.1 nm, b_1=4.35 nm, α_1=70°; a_2=b_2=4.18 nm, α_2=60° and a_3=2.4 nm, b_3=5.17 nm, α_3=75°). All these experiences were done at room temperature, at liquid-solid interface, using phenyloctane as solvent and graphite were used as substrate.

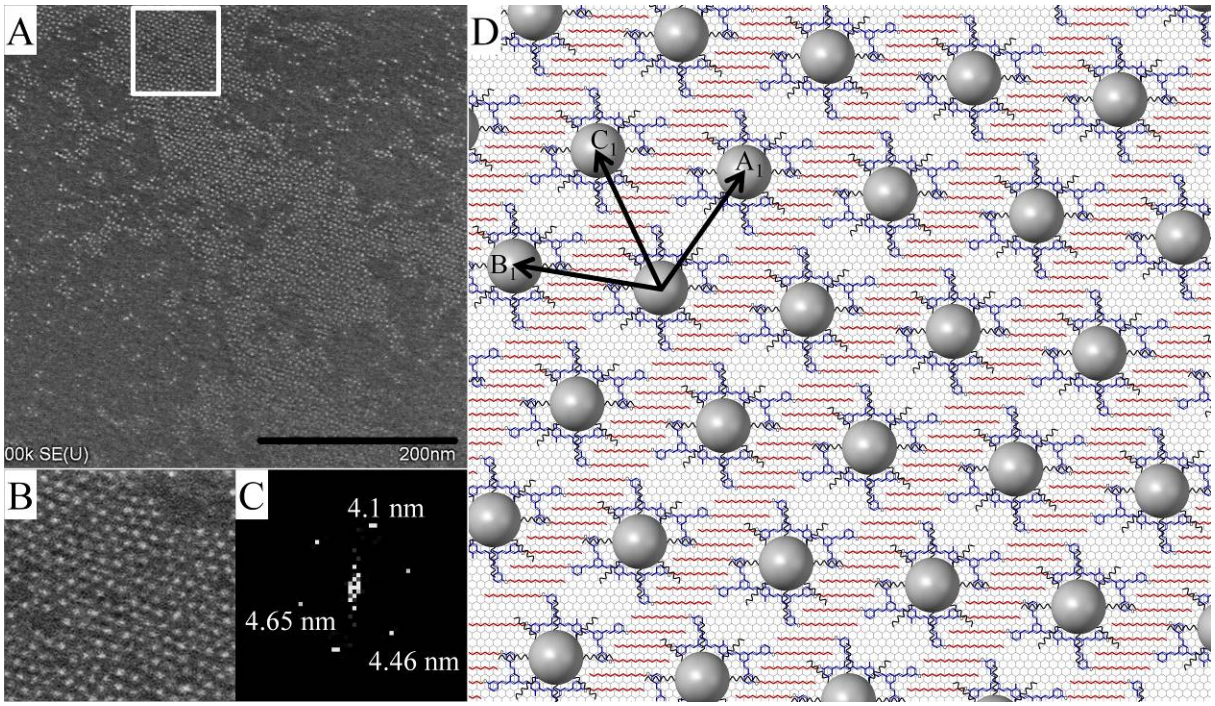

Figure 2. (A) HRSEM image (384x474 nm²) of Pt-$C_{18}NH_2$ nanoparticles deposited on the **G1-DSB-C_{14}** supramolecular template formed on the substrate; (B) zoom on a specified area (white square, 115x115 nm²) with an organization characterized by the (C) associated FFT; (D) Representation of the **G1-DSB-C_{14}** molecules self-assembled on graphite, oriented following the method detailed in ref. [19] and the suggested nanoparticle distribution inside this molecular matrix (A_1=4.2 nm, B_1=4.35 nm and C_1=4.65 nm).

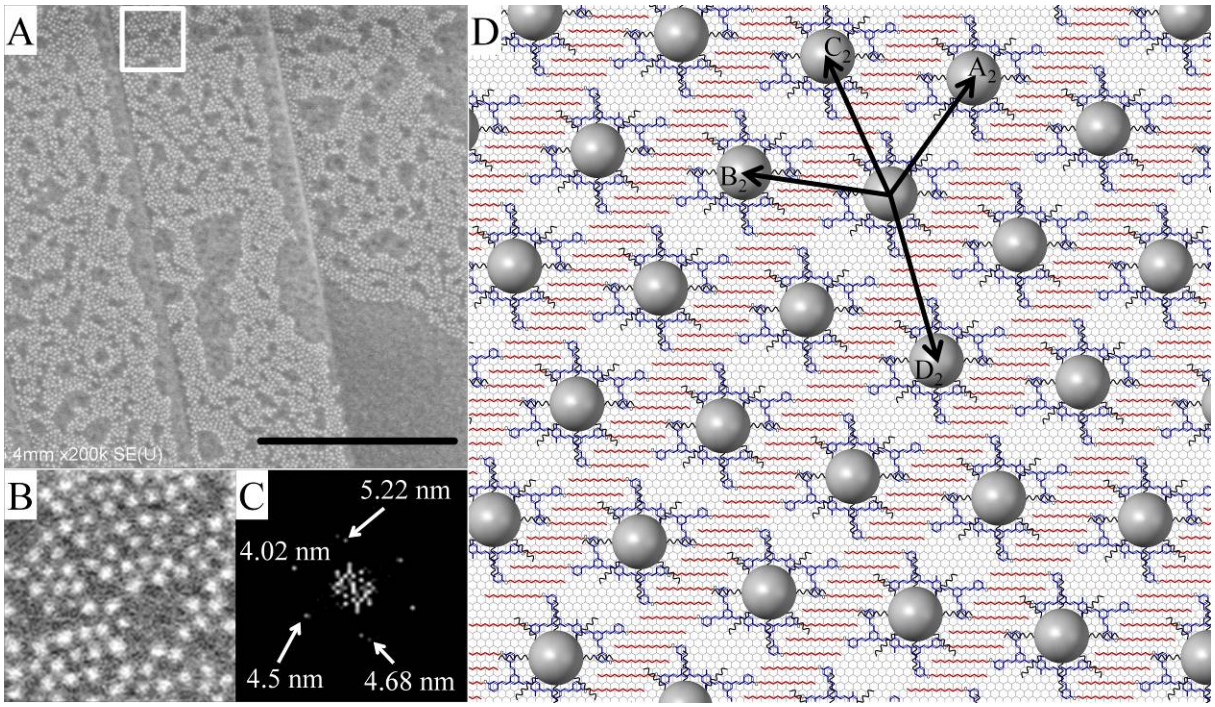

Figure 3. (A) HRSEM image (388x474 nm²) of Pt-$C_{18}NH_2$ nanoparticles deposited on the **G1-DSB-C_{14}** supramolecular template formed on the substrate; (B) zoom on a specified area (white square, 115x115 nm²) with an organization characterized by the (C) associated FFT; (D) representation of the **G1-DSB-C_{14}** molecules' considering a column shift (cf. Figure 1) self-assembly on graphite and the influence of this on nanoparticles' organization (A_2=4.2 nm, B_2=4.35 nm, C_2=4.65 nm and D_2=5.23 nm).

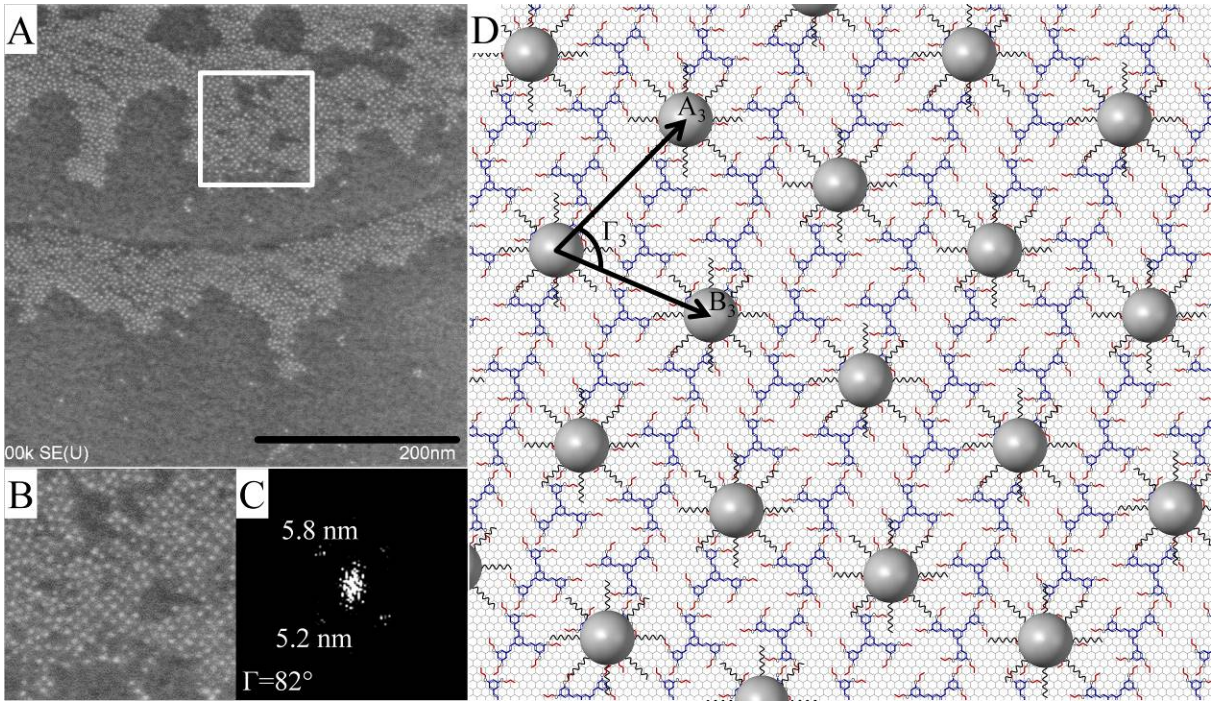

Figure 4. (A) HRSEM image (474x474 nm²) of Pt-$C_{18}NH_2$ nanoparticles deposited on the TSB-3,5-C_{12} supramolecular template formed on the graphite; (B) zoom on a specified area (white square, 115x115 nm²) with an organization characterized by the (C) associated FFT; (D) representation of the TSB-3,5-C_{12} molecules' self-assembly on graphite oriented following the method detailed in ref. [19] and the suggested nanoparticle distribution inside this molecular matrix (A_3=5.12 nm, B_3=6.00 nm and Γ_3=80°).

Table 1. Lattice parameters of the honeycomb structure and the linear organization β observed for the TSB-3,5-C_{12} molecules self-assembled on graphite.

Lattice parameters	Honeycomb network	Linear organization β
a_i [a)]	4.18 nm [b)]	2.4 nm
b_i [a)]	4.18 nm [b)]	5.17 nm
Γ_i [a)]	60° [b)]	75°

[a)] The subscript i is equal to 2 (respectively 3) for the honeycomb network (respectively the linear organization β); [b)] these values was taken from reference 17.

The table of contents

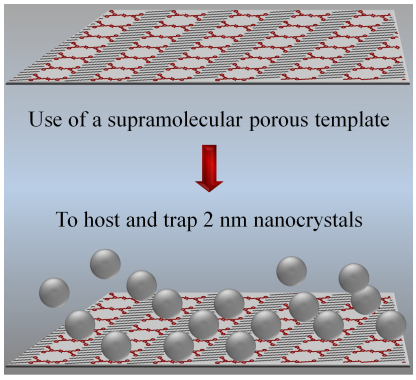

The pattern effect of a supramolecular network on assembly of metallic nanoparticles is demonstrated. The use of isotropic honeycomb and anisotropic linear porous supramolecular organic networks allow host 2nm Pt nanocrystals and to control both the geometry of the NCs organization and the interparticles distances.

Keyword: directed organizations, nanocrystals, supramolecular templates, self-assemblies at surfaces, nanoporous networks

Farid Kameche, Alice Six, Fabrice Charra, Anh-Tu Ngo, David Kreher, Caroline Salzemann, Fabrice Mathevet, Imad Arfaoui, André-Jean Attias*, Christophe Petit*

Title: Directed organization of platinum nanocrystals through organic supramolecular nanoporous templates.

Supporting Information

Directed organization of platinum nanocrystals through organic supramolecular nanoporous templates.

Farid Kameche [1,2,3], Alice Six[2], Fabrice Charra[3], Anh-Tu Ngo[1], Fabrice Mathevet [2], Caroline Salzemann[1], David Kreher [2], Imad Arfaoui[1],André-Jean Attias[2,], Christophe Petit[1,]**

1) Sorbonne Universités, UPMC Univ Paris 06, MONARIS, UMR CNRS 8233, 4 Place Jussieu, 75252 Paris Cedex 05, France.

2) Sorbonne Universités, UPMC Univ Paris 06, Institut Parisien de Chimie Moléculaire, UMR CNRS 8232, 4 Place Jussieu, 75252 Paris Cedex 05, France.

3) Service de Physique de l'Etat Condensé, CEA CNRS Université Paris-Saclay, CEA Saclay F-91191 Gif-sur-Yvette CEDEX, France.

Self-assembly and STM experiments.

Scanning tunneling microscopy (STM) images were acquired at room temperature with a homemade digital system. The self-assembly of the molecules was observed *in situ* at the liquid-solid interface. The fast-scan axis was kept perpendicular to the sample slope. All images were obtained in the height mode, *i.e.* with real-time current regulation. Images acquired simultaneously in both fast scan directions were systematically recorded and compared. The drift of the instrument was then corrected on these images by combining two successive images with downward and upward slow-scan directions, using specially

developed image cross-correlation software called Imago. The solvent was 1-phenyloctane (98%, Aldrich), which avoids the coadsorption often observed with linear alkanes. The substrate was HOPG (SPI, grade 2, 1×1×0.2 cm^3) and the tip was mechanically formed from a 250 μm Pt/Ir wire ($Pt_{80}Ir_{20}$, Goodfellow). The freshly-cleaved sample and tip quality was systematically checked by the STM observation of HOPG atomic network prior to molecular deposition. The self-assembled monolayers were formed by adding a droplet (ca. 5 μL) of the studied solution (**TSB-3,5-C_{12}** or **G1-DSB-C_{14}** molecules) on the substrate, immediately after observation of HOPG atomic network. Then, the self-assembled monolayers were observed by immersing the STM tip in the droplet.

The different main networks observed for the TSB-3,5-C_{12}

As mentioned on the article, the TSB-3,5-C_{12} self-assemble on graphite and according to the concentration, three organizations are mainly observed: for a concentration superior to 10^{-3} $mol.L^{-1}$, a linear compact structure α is observed (**Figure S1A**) while a honeycomb structure is preferentially formed for a concentration inferior to 5.10^{-5} $mol.L^{-1}$ (**Figure S1C**).[3,4] Moreover, a second linear compact structure (linear organization β) may coexist with the two other networks (**Figure S1B**).[3] The modification of the molecular arrangement is dependant of the concentration and also the stabilization of the molecules adsorbed: the most stable system is the one where adsorption energy by surface unit is the smallest possible.[5] According to the concentration, the number of molecules adsorbed on surface won't be equal and different geometries are less energetically costly. It drives then to observe different behaviours of the alkoxy peripheral chains and more specifically their adsorption on graphite. As shown on **Figure S1C_2**, the peripheral chains are positioned parallel to the graphite's surface. However, when the density becomes greater, the peripheral chains may be oriented towards the liquid as presented on **Figure S1A_2** (some chains are not fully represented).[4] Concerning the linear organization β, we cannot yet identified if all the chains are adsorbed or

not on the graphite. Besides, to put forward this phenomenon, the relative density was calculated using the lattice parameters reminded on **Table S1**, where the reference was the honeycomb structure (**Figure S2**). As expected, the linear organization α and β are denser 1.38 times and 1.25 times respectively than the porous network.

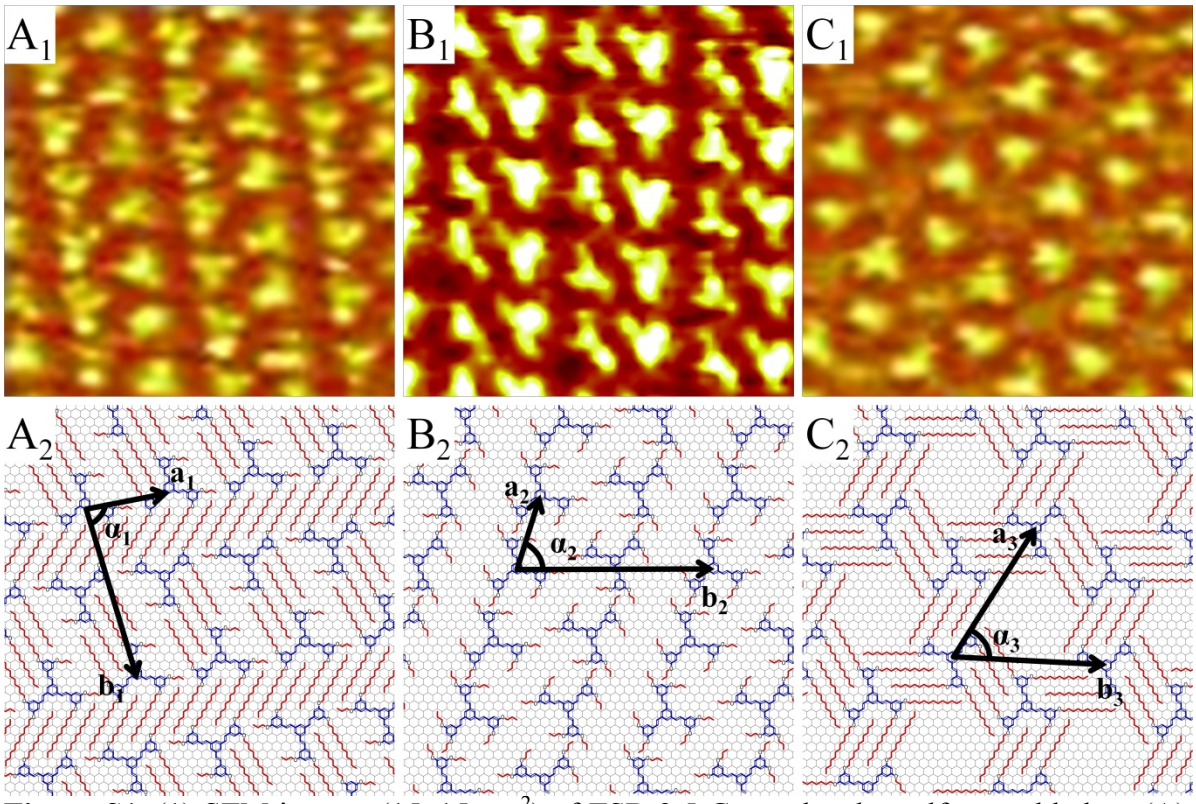

Figure S1. (1) STM images (15x15 nm^2) of TSB-3,5-C_{12} molecules self-assembled on (A) α compact network, (B) β compact network and (C) honeycomb (I=20 pA, V=-888 mV, C=$4.0x10^{-5}$ $mol.L^{-1}$). For all images, lattices parameters had been determined experimentally and used to determine (2) a representation of the TSB-3,5-C_{12} molecules' self-assembly on graphene

Table S1. Lattice parameters of the honeycomb structure, the linear organization β and the linear organization α observed for the TSB-3,5-C_{12} molecules self-assembled on graphite.

Lattice parameters	Linear organization α	Linear organization β	Honeycomb network
a_i [a)]	2.25 nm [b)]	2.4 nm	4.18 nm [b)]
b_i [a)]	4.94 nm [b)]	5.17 nm	4.18 nm [b)]
Γ_i [a)]	70° [b)]	75°	60° [b)]

[a)] The subscript i is equal to 1, 2 or 3 and refer respectively to the linear organization α, the linear organization β and the honeycomb network; [b)] these values were taken from[3,4].

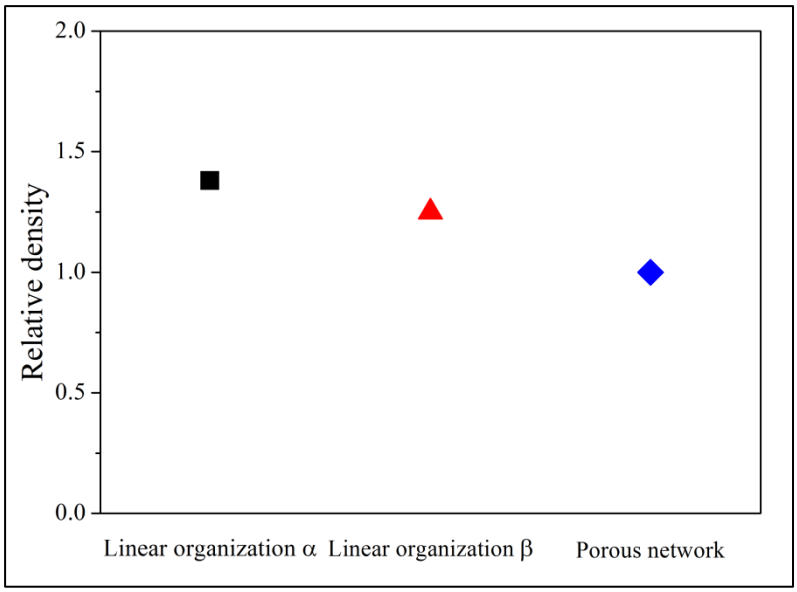

Figure S2. Graph comparing the molecular relative density of the three main networks observed for the TSB-3,5-C_{12}. The density of the porous network is here the reference and then equal to 1.

It is important to notify that a self-assembly can be observed by STM on a dried sample. Indeed, a sample was prepared to confirm that the self-assembly is still present once dried. For that, 10 µL of a solution of TSB-3,5-C_{12} at 10^{-6} mol.L^{-1} are dissolved on phenyloctane and once the solvent is evaporated, the sample is characterized by STM. Despite the difficulties to have a good resolution due to the absence of an insulating solvent, the observation of a honeycomb structures remains possible (**Figure S3A**). Plus, on different areas, a linear organization was discernible (**Figure S3B**). The formation of a linear compact is consistent with a high molecular density and then a higher concentration of TSB-3,5-C_{12} on the graphite surface. Regarding the concentration of the solution, a porous network should be preferentially formed. Yet, during the deposition of the solution on the substrate, the diffusion of the solution is not fast enough to get a local homogeneous concentration on the entire surface. This phenomenon drives then to have different local concentration and can justify the self-assembly of the TSB-3,5-C_{12} molecules into a compact organization.

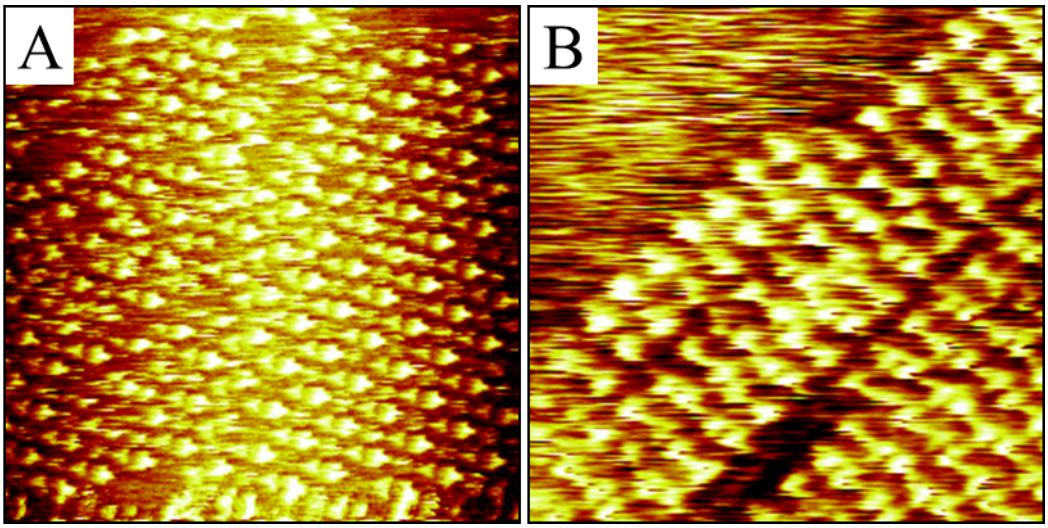

Figure S3. STM images of TSB-3,5-C_{12} molecules self-assembled on graphite (A) honeycomb network (60×60 nm^2, I=98 pA, V=-350 mV) and (B) a compact network (35×35 nm^2, I=20 pA, V=-990 mV). Here the characterization was done on a dried sample.

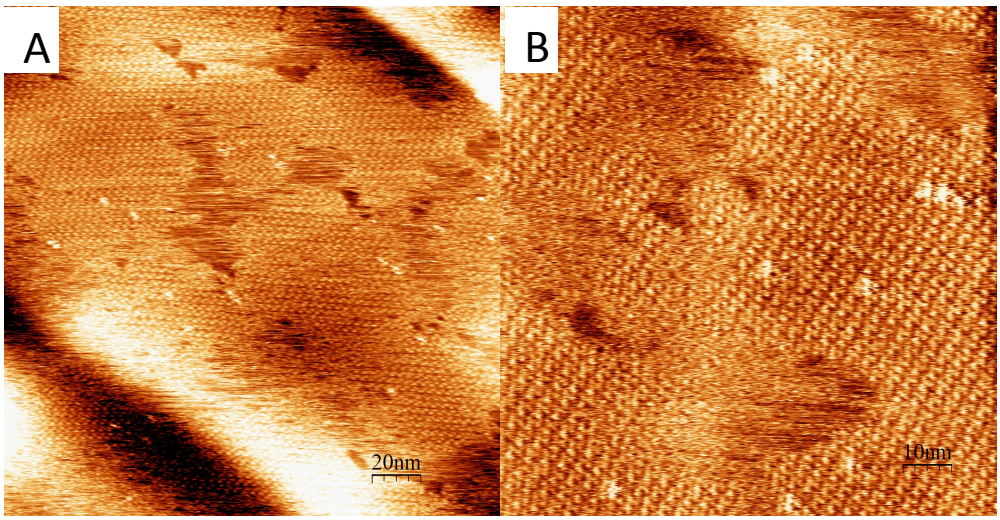

Figure S4. STM images at solid/air interfaces of TSB-3,5-C_{12} molecule self-assembled on HOPG substrates after drying of the solution (A) 200×200 nm^2, I=20 pA, V=-1V. The honeycomb structure is clearly visible at high magnification (B) 100×100 nm^2, I=20 pA, V=-1V .

Synthesis of Pt-$C_{18}NH_2$ nanoparticles.

Initially developed by Brust *et al.,*[6] this synthesis was already used on the laboratory to form monometallic nanoparticles (Pt[7,8] and Pd[9,10]) and bimetallic nanoparticles (CoPt[11–13] and PdPt[13,14]). First, the precursor, $PtCl_6^{2-}$, is formed *via* a complexation reaction between hydrochloric acid and platinum(IV) chloride on water under stirring during one hour. At the same time, a solution of tetrakis(decyl)ammonium bromide (TDAB) dissolved on 40 mL of

toluene by ultrasonic bath is prepared. Afterwards, the transfer of the precursor on the latter solution is ensured by a vigorous stirring during two hours. The organic phase is then isolated and 1.5 mL of oleylamine is added to it. An aqueous solution of $NaBH_4$ (5 mmol in 12.5 mL of water), which was under stirring during 20 minutes, is soon after slowly added to the precursor's solution under agitation for 24 hours (**Figure S5**). Lastly, the organic phase is extracted to evaporate the toluene and to wash the nanoparticles with ethanol in combination with centrifugation. A good solvent - $CHCl_3$ is chosen here but toluene or an alkane may be used too – is then added to solubilize Pt-$C_{18}NH_2$ nanoparticles.

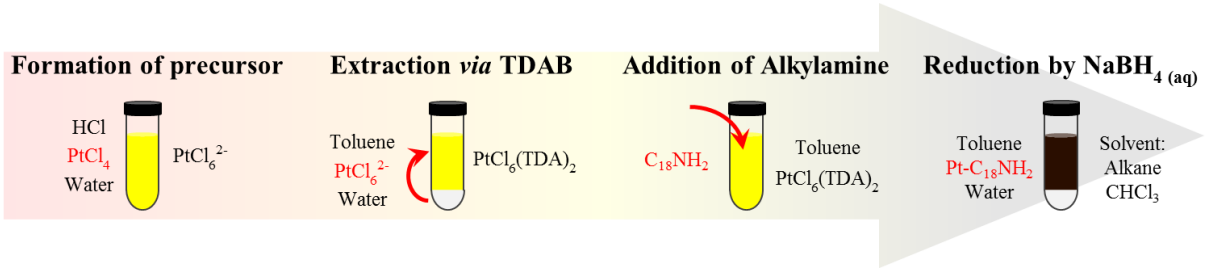

Figure S5. Scheme of the liquid-liquid phase transfer synthesis' protocol.

Characterization of Pt-$C_{18}NH_2$ nanoparticles

To determine the size and polydispersity of the nanoparticles we perform a characterization by Transmission Electronic Microscopy (TEM, JEOL 1011). A TEM copper grid, covered by a thin film of amorphous carbon, is placed on a filter paper and 10 µL of the solution is deposited on the grid. Few images with a magnification at 80000 are taken (**Figure S6A**) and the size distribution is determined (**Figure S6B**) with two softwares: ImageJ and Excel.

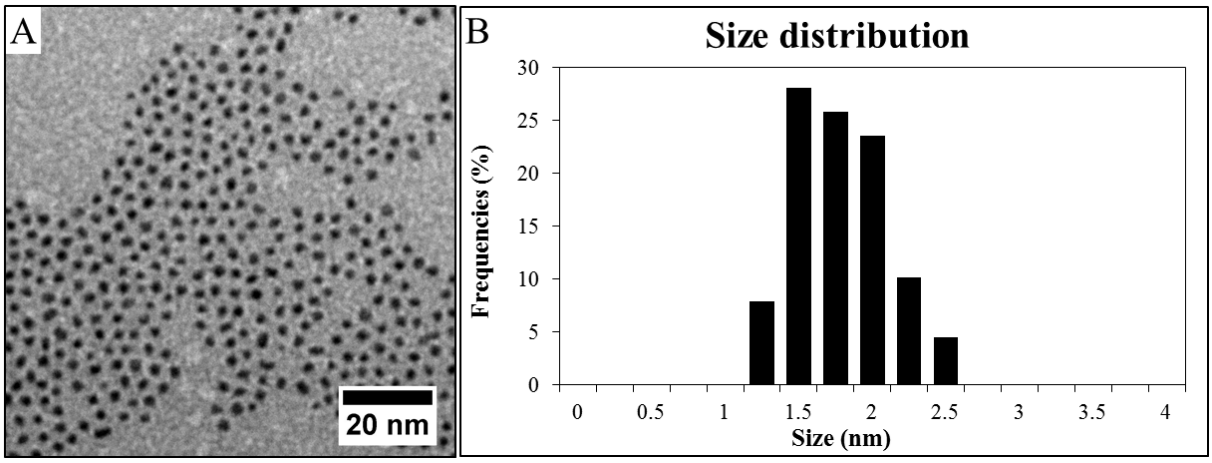

Figure S6. (A) TEM image and (B) size distribution of Pt-$C_{18}NH_2$ nanoparticles.[14]

Once the nanoparticles are synthesized and characterized, a control sample is prepared as described on the article: on a freshly cleaved graphite, 10 µL of the Pt-$C_{18}NH_2$ at 10^{-6} mol.L^{-1} is dropped on the substrate. Once dried, the sample is characterized by High Resolution Scanning Electronic Microscopy (HRSEM) via a Hitachi SU-70 Microscope. A typical HRSEM image is shown on **Figure S7A** where there is no obvious organization (**Figure S7B**) and illustrated by the Fast Fourier Transform (FFT) on **Figure S7C**.

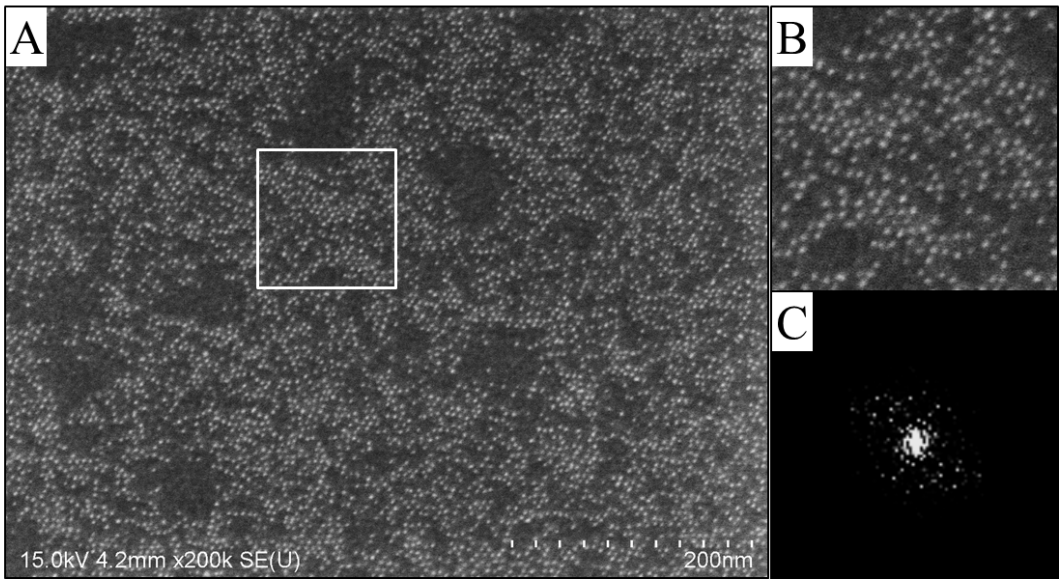

Figure S7. (A) HRSEM image of the control sample; (B) zoom on an area (white square) where the organization is characterized by (C) the FFT.[14]

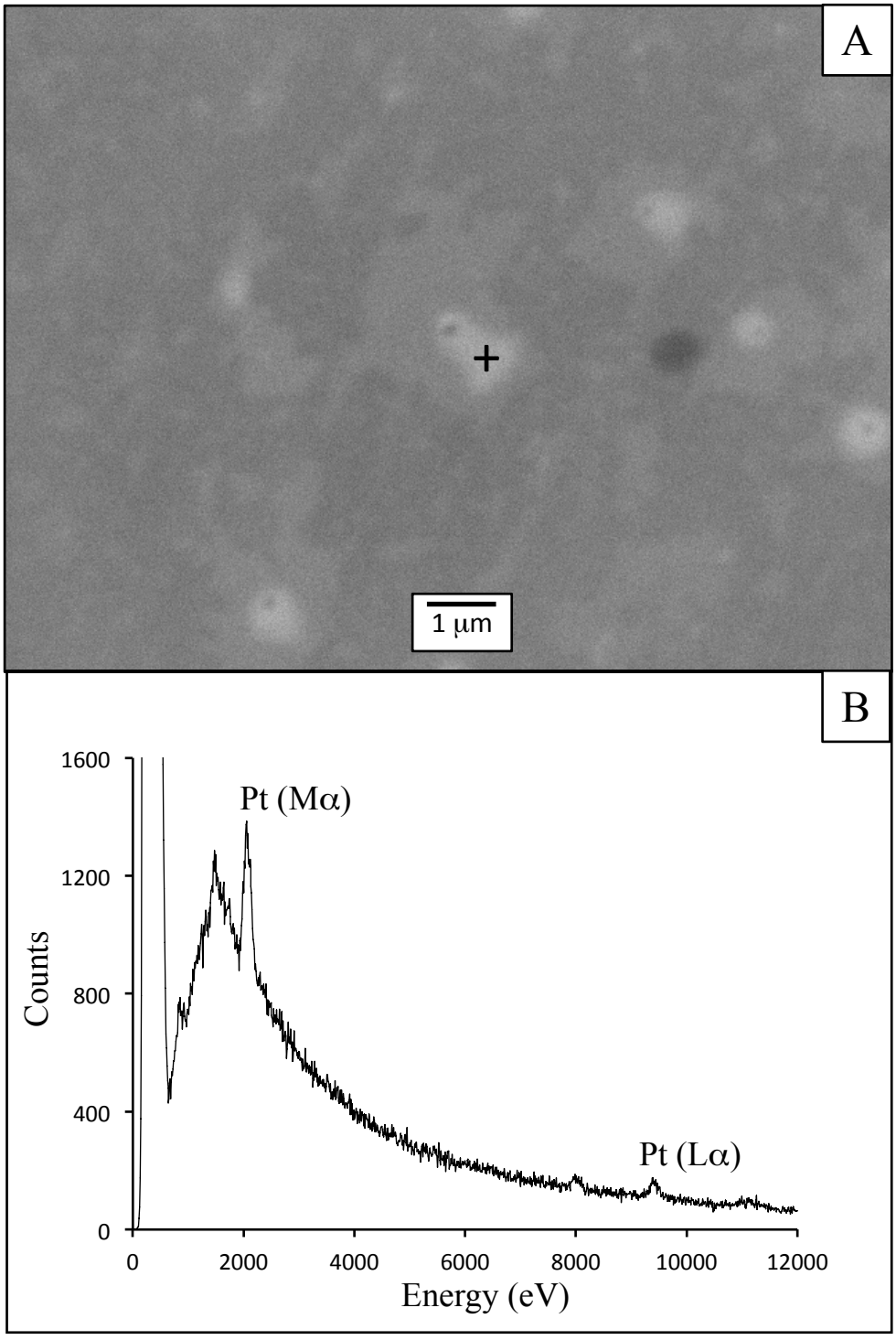

Figure S8. (A) Low magnification SEM image of the control sample; (B) EDX analysis of zone 1 (marked with a +)

Reference

[1] S. K. Deb, T. M. Maddux, L. Yu, *Journal of the American Chemical Society* **1997**, *119*, 9079.

[2] R. Ando, H. Ono, T. Yagyu, M. Maeda, *Inorganica Chimica Acta* **2004**, *357*, 817.

[3] C. Arrigoni, *Degree Thesis*, University Pierre and Marie Curie, May, **2010**.

[4] A. Bellec, C. Arrigoni, G. Schull, L. Douillard, C. Fiorini-Debuisschert, F. Mathevet, D. Kreher, A.-J. Attias, F. Charra, *The Journal of Chemical Physics* **2011**, *134*, 124702.

[5] F. Charra, J. Cousty, *Physical review letters* **1998**, *80*, 1682.

[6] M. Brust, M. Walker, D. Bethell, D. J. Schiffrin, R. Whyman, *Journal of the Chemical Society, Chemical Communications* **1994**, 801.

[7] K. Wikander, C. Petit, K. Holmberg, M.-P. Pileni, *Langmuir* **2006**, *22*, 4863.

[8] A. Demortière, P. Launois, N. Goubet, P.-A. Albouy, C. Petit, *The Journal of Physical Chemistry B* **2008**, *112*, 14583.

[9] K. Naoe, C. Petit, M. P. Pileni, *Journal of Physical Chemistry C* **2007**, *111*, 16249.

[10] C. Salzemann, C. Petit, *Langmuir* **2012**, *28*, 4835.

[11] A. Demortière, C. Petit, *Langmuir* **2007**, *23*, 8575.

[12] A. Demortière, C. Petit, *Journal of Applied Physics* **2011**, *109*, 84344.

[13] C. Salzemann, F. Kameche, A.-T. Ngo, P. Andreazza, M. Calatayud, C. Petit, *Faraday Discuss.* **2015**, *181*, 19.

[14] F. Kameche, *Degree Thesis*, University Pierre and Marie Curie, September, **2015**.